Available online at www.sciencedirect.com

SCIENCE DIRECT®

Earth and Planetary Science Letters 236 (2005) 227–237

EPSL

www.elsevier.com/locate/epsl

Seismic constraints on temperature of the Australian uppermost mantle

Saskia Goes[a,*], Frederik J. Simons[b], Kazunori Yoshizawa[c]

[a]*Institute of Geophysics, ETH Zurich, Switzerland*
[b]*Department of Earth Sciences, University College London, UK*
[c]*Division of Earth and Planetary Sciences, Hokkaido University, Sapporo, Japan*

Received 4 February 2005; received in revised form 25 April 2005; accepted 2 May 2005
Available online 20 June 2005
Editor: S. King

Abstract

We derive estimates of temperature of the Australian continental mantle between 80 and 350 km depth from two published *S*-velocity models. Lithospheric temperatures range over about 1000 °C, with a large-scale correlation between temperature and tectonic age. In detail however, variations ranging from 200 to 700 °C occur within each tectonic province. At the current seismic resolution, strictly Proterozoic and Archean blocks do not have substantially different temperatures, nor does the Phanerozoic lithosphere east and west of the Tasman line. Temperatures close to an average (moist) MORB source mantle solidus characterize the eastern seaboard and its offshore. Differences between the temperatures derived from the two velocity models illustrate the importance of well-constrained absolute velocities and gradients for physical interpretation. The large range of lithospheric temperatures cannot be explained solely with documented variability in crustal heat production, but requires significant variations in mantle heat flow as well.

Keywords: temperature; lithosphere; continent; surface wave velocity; Australia

1. Introduction

Temperature controls fundamental properties of the Earth's lithospheric mantle such as density, rheology, and thermal conductivity. While oceanic lithosphere largely behaves as a cooling thermal boundary layer, the role of continental lithosphere in modulating the release of mantle heat remains poorly understood [e.g., [1–3]]. It is debated to what extent continental lithospheric temperatures correlate with thermo-tectonic age, and what the relative importance is of crustal heat production and heat supplied from greater depths in the lithosphere and mantle [4,5].

* Corresponding author. Current address: Department of Earth Science and Engineering, Imperial College London, South Kensington Campus, London, SW72AZ, UK. Tel.: +44 20 759 46434; fax: +44 20 759 47444.
E-mail address: s.goes@imperial.ac.uk (S. Goes).

0012-821X/$ - see front matter © 2005 Elsevier B.V. All rights reserved.
doi:10.1016/j.epsl.2005.05.001

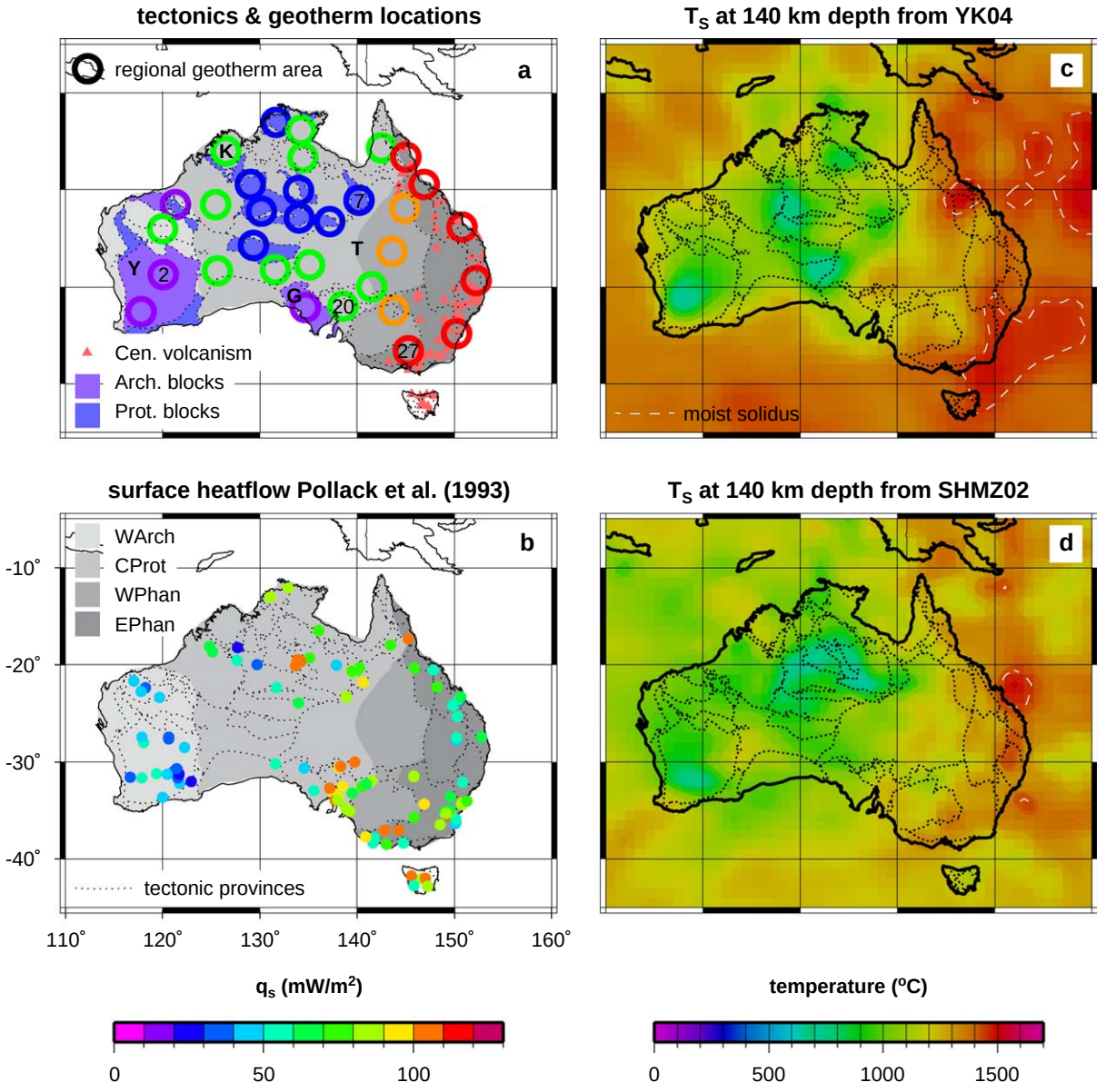

Fig. 1. (a) Tectonic map of Australia, showing tectonic provinces (dashed lines) and locations of Cenozoic volcanism (red triangles). Also shown is the large-scale tectonic/thermal subdivision: Archean, Proterozoic, western and eastern Phanerozoic, in increasingly darker gray shades [after [14,22]]. The coarse tectonic division and the circles were used for calculation of the average geotherms in Fig. 3a,b,c, respectively. Colors correspond to tectonic affiliation: purple—Archean, blue—Proterozoic, orange, red—Phanerozoic non-/volcanic (see legend Fig. 3). Y—Yilgarn craton, K—Kimberley, G—Gawler craton, T—Tasman Line. (b) Australian surface heat-flow data from the Pollack et al. compilation [15], which give a good indication of the distribution and values of heat-flow measurements. (c) Map of temperature at 140 km depth, inferred from the V_S model of [23], assuming a constant pyrolite composition. (d) Similar as (c), but inferred from the V_S model of [21]. White-dashed contours mark the moist MORB-source solidus of Hirth and Kohlstedt [31].

Surface heat flow directly reflects the lithosphere's thermal state, but its extrapolation to temperature at depth involves many uncertainties [6,7], and requires the assumption that heat transport is conductive and in steady-state. Seismic velocities provide in situ information on lithospheric mantle structure, and are strongly sensitive to temperature in the uppermost mantle. Basaltic depletion of lithospheric mantle—which is thought to increase with thermo-tectonic age [8]—may cancel thermal effects on density [9], but the effect of such compositional variations on seismic wave speed is secondary to that of temperature [10,11]. Joint inversions of gravity and seismic data have hinted at compositional variability in the lithosphere [12,13]. However, such approaches carry larger uncertainties than the ones with which we can determine thermal structure from regional seismic models at the current resolution, when compositional influence is neglected. Such seismic temperature estimates are derived here for the Australian uppermost mantle.

The Australian continent comprises tectonic domains ranging from Archean cratons in the west, Proterozoic metamorphic belts in the center, to Mesozoic basins that have experienced Cenozoic volcanism in the east (Fig. 1a). Compared to North America and Europe, there is limited information about the thermal structure of its lithosphere, as heat-flow data are sparse [14,15] (Fig. 1b). Data for the western and eastern parts of the continent fall within global trends of how heat flow generally decreases with tectonic age. In contrast, the predominantly Proterozoic center of the continent is characterized by surface heat flow significantly higher than global averages (which are dominated by the densely sampled European and North American continents) [16,17]. In a few locations, geothermobarometry provides temperature-depth profiles that indicate cool conditions under the Proterozoic domains and non-steady state thermal conditions in southeastern Australia, associated with Cenozoic volcanism [18].

Both body and surface-wave studies reveal a lithosphere that is fast under the western two-thirds of the continent and relatively slow under the eastern rim, with seismic thicknesses of up to 300 km [19–24]. Here, we analyze the recent *S*-velocity models of Simons et al. [21] and Yoshizawa and Kennett [23]. Both velocity models are based on multimode Rayleigh-wave dispersion analyses, but use different inversion techniques and theoretical approximations. Surface-wave data have yielded continental-scale velocity models for several other continents with a lateral and radial resolution appropriate for tectonic interpretation [e.g., [25]]. Unfortunately, no *P*-velocity model of similar resolution exists for Australia. The distribution of data used in the two *S*-velocity models is similar, so differences between the models provide information on the uncertainties inherent to tomographic inversions. Together with the published model resolution estimates this gives a more complete picture of the seismic resolution. The seismically derived temperatures we obtain are compared with independent constraints from surface heat flow and geothermobarometry.

2. Velocities and temperature conversion

The velocity model of Simons et al. [21] is based on a partitioned waveform inversion of constraints derived from fundamental Rayleigh waves with 40–200 s periods and higher modes with periods between 20 and 125 s along over 2200 paths sampling most of the Australian continent. With such data, the bulk of the mantle-structure resolution is confined to depths between 80 and 400 km. Although model resolution is notoriously hard to quantify, numerous tests and comparisons between modeling techniques indicate a nominal resolution of 250 km laterally and 50 km radially [21]. Wave speed perturbations are believed to be accurate within 0.75% of the background model [21]. Thermal interpretation only requires the isotropic part of this model (which also included azimuthal anisotropy). We will subsequently refer to this model as SHMZ02.

The model of Yoshizawa and Kennett [23] uses a three-step inversion method. First, multi-mode phase speeds of Rayleigh waves are derived from the 2000 1-D path-specific shear-speed profiles determined by Debayle and Kennett [20]. The spatial coverage, controlled by the distribution of sources and receivers, is similar as in model SHMZ02. In the second step, they invert the path-specific phase speeds for dispersion maps of the fundamental mode and three higher modes, for period ranges between 40 and 150 s. Higher frequencies, which are increasingly affected by (unmodeled) mode coupling, were not considered. In this step, the effects of off-great-circle propagation

and finite frequency of surface waves are incorporated. In the final step, the set of dispersion maps for several modes and frequencies are combined to construct 3-D shear speeds. The authors estimate their horizontal resolution at 400 km. The model is reliable down to about 350 km depth, with a depth resolution that is on the order of 50 km. The recovery of velocity anomaly amplitudes is likely somewhat better than in models where finite-frequency effects are neglected [23,26]. This (isotropic) model will be given the acronym YK04.

Our approach to convert velocities between 80 and 350 km into temperature is a slightly updated form of the procedure of Goes et al. [10]. It accounts for both elastic and anelastic effects. All elastic parameters are taken from the compilation by Cammarano et al. [27]. The anelasticity model used for the displayed results is model Q_1 [10]. The elastic parameters are extrapolated linearly to high temperature and using 3rd order finite strain to high pressure [27]. Because of the non-linear temperature dependence that anelasticity introduces at shallow mantle depths, absolute velocities (not just anomalies) are required for a thermal interpretation [10,27]. Using this method, we found that when we assume that velocity structure is the result of temperature variations only, *P*-velocities, *S*-velocities and surface heat flow for the uppermost mantle under Europe and North America yield consistent temperature estimates [10,28]. This confirms that composition has a secondary effect on seismic structure at shallow mantle depths. It should be noted however that neither of the models used for North America and Europe samples typical cratonic areas, where depletion is largest [8], and most noticeable due to lower temperature sensitivity of seismic waves at low temperature [10].

Unless noted otherwise, we assume a pyrolite composition and include all phase changes below the spinel–garnet transition [29]. In our previous work, we used a linear depth extrapolation and neglected all phase transitions. The non-linear extrapolation with depth and the inclusion of olivine- and garnet-component phase transitions (mainly the gradual pyroxene–garnet solid solution in the depth range of interest here) turn out to have only a minor effect (at most few 10s of degrees) on the temperatures inferred. The (not-included) spinel–garnet transition at around 60–80 km depth has a somewhat larger velocity signature than the deeper garnet transitions. Neglecting it adds only a small uncertainty because of the very strong temperature-sensitivity at these depths [10]. Uncertainties in the elastic and anelastic mineral parameters, by themselves, result in temperature estimates with confidence intervals of ± 100 °C [10,27].

3. Thermal structure

3.1. Seismic temperatures

Temperatures at 140 km depth range over 1000 degrees, from 500–600 °C to 1500–1600 °C (Fig. 1c,d, Fig. 2). The lowest temperatures are found under the North Australian "craton", an assemblage of Proterozoic domains in north-central Australia, and

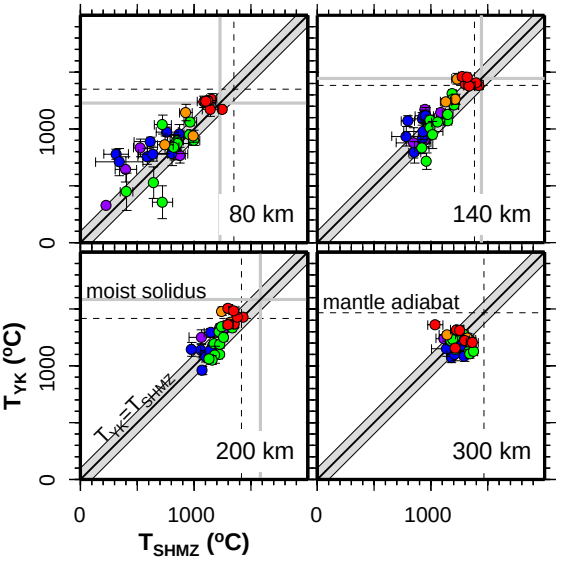

Fig. 2. Comparison of temperature estimates from the two *S*-velocity models (Simons et al. [21]—SHMZ02, and Yoshizawa and Kennett [23]—YK04) at several depths. Dots (colored according to tectonic affiliation, see legend in Fig. 3) represent temperature averages over the circles in Fig. 1, with error bars corresponding to the variation within the circle. In bold, the line $T_{YK}=T_{SHMZ}$ is shown, flanked by a gray ± 100 °C zone illustrating the uncertainty in the V_S–temperature conversion. Dashed lines mark the temperature of an adiabat with a 1300 °C potential temperature, gray lines the MORB-source solidus of Hirth and Kohlstedt [31]. There is a strong correlation between the two thermal fields, but small systematic differences in temperatures at the shallowest and largest depths. The range in temperature is similar in both models.

under the Archean Yilgarn craton. The highest temperatures are found below the eastern seaboard and the adjacent oceanic domains. A strongly depleted cratonic composition [8] would increase the lowest temperatures by about 200 °C, while the highest temperatures would barely be affected [10,28].

Despite their different inversion procedures and theoretical approximations, both *S*-velocity models yield a very similar range and large-scale distribution of temperature, and temperature estimates correlate well (Figs. 1 and 2). However, the YK04 model systematically gives somewhat higher temperatures than the SHMZ02 model above 200 km depth (Figs. 1 and 2), and somewhat lower than SHMZ02 temperatures below 200–250 km (Figs. 2 and 3). These differences may reflect the reference models towards which the seismic inversions are damped. At depths shallower than about 200 km, SHMZ02's reference velocities exceed those of YK04's reference model; at larger depths, the relation reverses. Below, we discuss the features of the temperature field that emerge as robust from both models. Discrepancies between the temperatures derived from the two models can be attributed to differences in inversion technique and spatial resolution. This illustrates how uncertainties in the absolute seismic velocities can affect physical interpretation.

On average, there is a systematic decrease of temperature with thermo-tectonic age (Fig. 3). A similar first-order correlation has been noted for Australian average seismic velocity, seismic lid thickness and mechanical strength [30]. The trend is illustrated by the large-scale thermal averages (Fig. 3a) over the main tectonic/heat-flow provinces (Fig. 1), i.e. the Archean west, the mainly Proterozoic center, and the Phanerozoic east. The latter is further subdivided into an eastern part, which has been affected by Cenozoic volcanism, and an unaffected western part. At 140 km depth, the continent's center is about 100 °C warmer than the Archean west, and the Phanerozoic east is almost 500 °C warmer than the center (Fig. 3a). The highest temperatures, close to the solidus representative for a (moist) MORB source [31], are found near the eastern seaboard (Fig. 1). These temperatures are similar to the, also resolved, oceanic temperatures northwest of Australia.

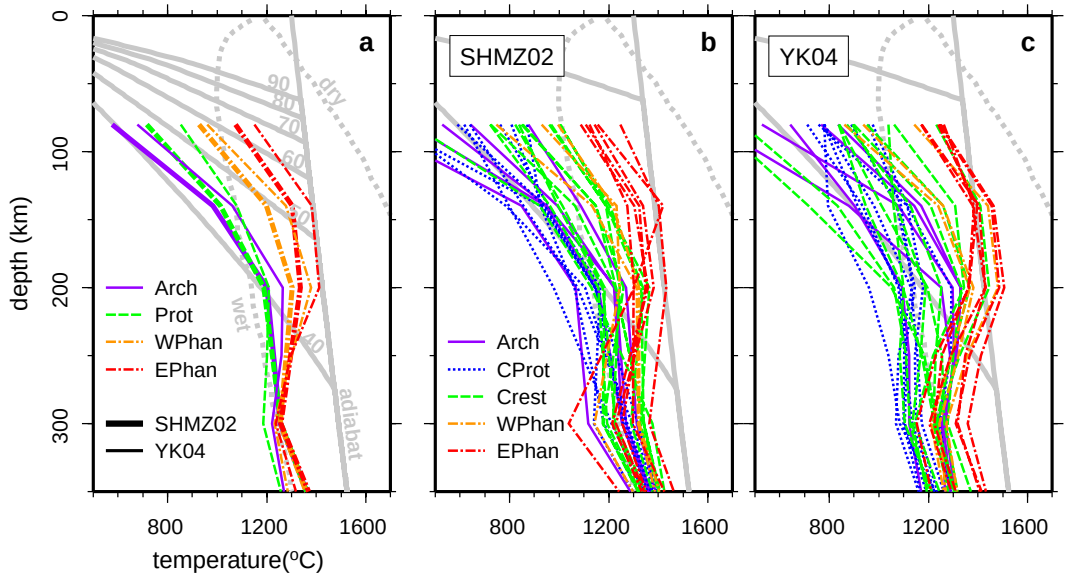

Fig. 3. (a) Average geotherms for the large-scale tectonic subdivision (see Fig. 1). Thick lines are from the model of Simons et al. [21] (SHMZ02), thin lines from the model of Yoshizawa and Kennett [23] (YK04) (b) Geotherms for circles with 300 km diameter, indicated on Fig. 1, from temperatures of model SHMZ02. (c) As (b), but inferred from model YK04. For reference, solid gray lines show steady-state geotherms from Chapman [6], labeled with their corresponding surface heat-flow values, and a 1300 °C mantle adiabat, as well as the wet and dry peridotite solidi [56].

As observed for mechanical and seismic thickness [30], our mantle temperatures show notable regional deviations from an age-dependent pattern, on scales smaller than about 1000 km. To investigate the thermal structure in more detail, while respecting the lateral seismic resolution, regional geotherms (Fig. 3b,c) were determined by averaging temperature over circles with 300 km diameter. Their locations were chosen to correspond to tectonically and thermally interesting points and they are spread over the continent (Fig. 1). The circles' size is small enough that each one is mostly contained within a single tectonic block. By color, we distinguish the geotherms according to their tectonic affiliation. Besides the coarse division made before (Archean, Proterozoic, west and eastern Phanerozoic), we divided the geotherms of the central part into those corresponding to Proterozoic blocks and those falling in the area in between, and the small Archean Gawler craton located in the southeastern corner of the central tectonic province.

The regional geotherms (Fig. 3b,c) show that the Proterozoic geotherm in Fig. 3a is the average of two components, the actual Proterozoic domains, which have temperatures as low as the Archean cratonic blocks, and the area in between, which overlaps in temperature with the geotherms from the western part of the Phanerozoic domain. Very low cratonic temperatures around 80 km depth would be raised about 200 °C [10] by accounting for a strongly depleted composition [8]. Resolution below the Yilgarn craton is significantly less than that under north-central Australia and apparent differences in thermal thickness between these regions are probably not resolved [21,23,24].

Three of the coldest central Australian geotherms do not strictly fall within the Proterozoic blocks, yet they follow Proterozoic/Archean profiles (Figs. 2 and 3). Differences between the geotherms according to the two seismic models, sometimes amounting to several 100 °C (Figs. 2 and 3), also reflect that 300 km is at the small-scale limit of the spatial resolution. Yet, the ensemble of regional geotherms gives a good overview of temperature deviations. Within each tectonic domain there are thermal variations of 200 °C (EPhan, WPhan) to about 700 °C (Arch, Prot and the rest of the central tectonic province). Temperatures in the eastern part of the Phanerozoic province are all higher than in the rest of the continent and are the only ones to approach the 1300 °C mantle adiabat.

3.2. Lithospheric thickness

The large-scale tectonic geotherms converge at 300 km (Figs. 2 and 3a), although wave speeds in both models are constrained to larger depths. This indicates that the thermal thickness of the conductive lithosphere is about 300 km. By this depth, the overall temperature range has halved, to about 500 degrees, with temperatures between 900–1000 °C and 1500–1600 °C (Figs. 2 and 3). Tracing the depth of a 1200 °C isotherm (often taken as a proxy for the thermal base of the lithosphere) is made somewhat difficult by the varying thermal gradients with depth, but also yields depths of around 300 km under the west and central tectonic provinces and depths ranging from 150 to 200 km under the western Phanerozoic to less than 100 km in the east. Similar thermal thicknesses were independently obtained from surface heat-flow data [32]. These estimates are also consistent with the seismic thickness, which, when defined as the depth of the 1% velocity anomaly contour, lies at 250–300 km [30]. Whereas at depths shallower than 250 km seismic structure clearly correlates with surface tectonics, this correlation has all but disappeared below 300 km depth.

Note that the geotherms at depth do not converge to the adiabat taken to be representative of convective-mantle temperatures (Figs. 2 and 3). A potential mantle temperature of around 1300 °C has been inferred from petrologic data [33] and the correspondence of olivine-system phase transitions with the 410 and 660 km discontinuities [34]. It could be somewhat higher [35], but is unlikely to be significantly lower. The equation of state we used, as well as the incorporation of garnet-component phase transitions, which start above 400 km, do not significantly influence the recovered temperatures at these depths. Other continental velocity models have yielded similarly cool sublithospheric temperatures [10,28]. These low temperature estimates may be controlled by the used background velocity models, which are not strongly seismically constrained [27,36]. Shapiro and Ritzwoller [37] found that, besides models damped towards global seismic reference models, velocity structure compatible with the mantle adiabat were also acceptable solutions to their uppermost-mantle surface-wave tomography. Such uncertainties in the absolute velocity structure, as

well as uncertainties in the extrapolation of anelasticity with depth [38] need to be further investigated before an interpretation of the deep subcontinental temperatures can be made.

3.3. Comparison with other data

The geotherms are compared with a standard set of steady-state conductive geotherms inferred from global surface heat-flow studies [6]. These geotherms assume that 40% of the surface heat flow is produced in the continental crust and 60% (the reduced or mantle heat flow) is supplied from below (lower crust, lithosphere and mantle). The Archean west has temperatures that are close to those of such a 40 mW/m^2 geotherm (Fig. 3a), compatible with the low heat flow, 39 ± 8 mW/m^2, measured in this part of the continent [16] (see also Fig. 4, area 2). The Phanerozoic east has temperatures that join those of 60–70 mW/m^2 geotherms (Fig. 3a), consistent with the average surface heat flow of 72 ± 27 mW/m^2 observed there. The lithospheric temperatures of the Proterozoic center are much lower than expected from extrapolation of its average surface heat flow of 82 ± 25 mW/m^2 [16] along these standard geotherms. Instead, they are more compatible with a geotherm anchored to the global Proterozoic heat-flow average between 49 and 54 mW/m^2.

It should be noted that heat-flow data coverage is fairly sparse [14–16] (Fig. 1b). Within the uncertainties, heat-flow derived temperatures agree with the seismic temperatures in most locations where both are available. Exceptions are the few very high (>90 mW/m^2) heat-flow locations in central Australia (e.g. at circle 7, Fig. 4). The high central Australian average heat flow is influenced by these values, whose origins lie in anomalously high values of crustal heat production, as previously inferred from geochemical analyses [16,17]. A large variation in lithospheric temperatures in the central and eastern tectonic provinces is consistent with the large variations in heat flow (both cases ± 25 mW/m^2) in these two provinces.

Temperatures under the Kimberley province in north-central Australia and Gawler craton are somewhat higher than the temperatures close to a 40 mW/m^2 conductive geotherm inferred from garnet concentrates [18], but consistent with the few available heat-flow measurements. Temperatures in southern Australia (Fig. 4, circle 20) are consistent with the strongly concave cratonic-margin xenolith geotherm (EMAC) [18]. The moderate crustal heat-flow values along the east coast agree with the mantle temperatures that are

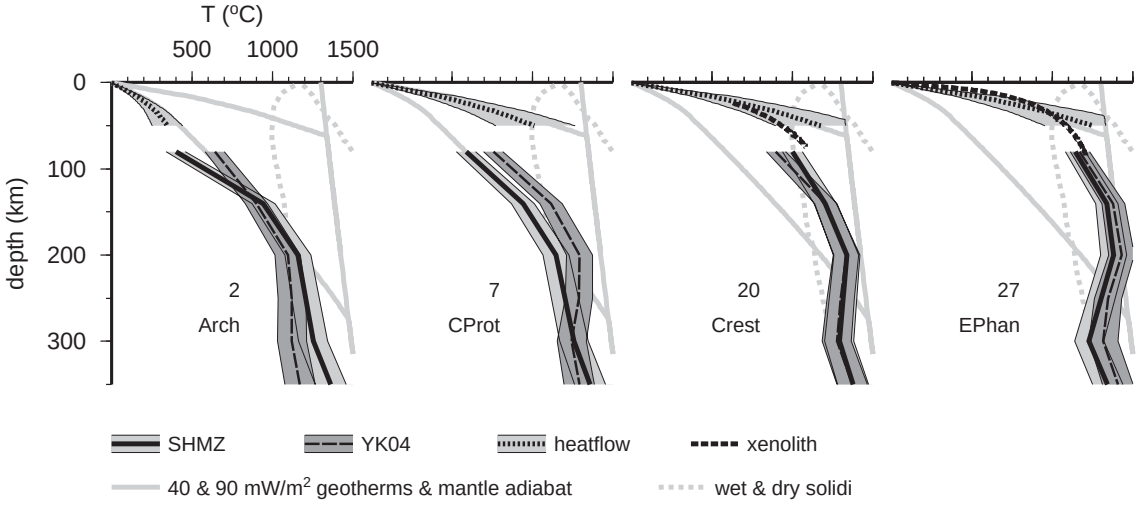

Fig. 4. Comparison of seismic geotherms (with uncertainties according to Cammarano et al. [27], bold solid lines with light gray uncertainties—SHMZ02, long-dashed lines with dark gray uncertainties—YK04) with surface heat flow (shallow geotherms calculated following [6], with ±20% uncertainty, bold dotted lines with light gray uncertainties) and geotherms from geothermobarometry (short-dashed bold lines, [18]) for a selection of the geotherms in Fig. 2b (locations labeled in Fig. 1). For reference, gray lines show the 40 and 90 mW/m^2 geotherms according to [6], and a 1300 °C mantle adiabat, as well as the wet and dry peridotite solidi [56] (dotted).

high for the Australian continent but not as high as under tectonically active regions in the western US and parts of west and central Europe [10,28]. Locally higher values, e.g. under southeastern Australia may be due to non-steady state thermal structure associated with the recent volcanism. The geothermobarometry profile [39] derived for this region is able to reconcile high surface heat-flow values with the moderate mantle temperatures and steep thermal gradients that we infer (Fig. 4, circle 27).

4. Discussion

4.1. Seismic resolution

The results indicate what aspects of the seismic models would need refinement for better temperature constraints. Enhanced lateral resolution will be helpful, and is already strived for in most tomographic models. It can be achieved by denser data coverage, and by combining different data types, e.g., surface and body wave data, group and phase velocities, waveform data and polarization constraints, or seismic and other geophysical data, for example from geothermobarometry on xenoliths [40–43].

Also important, however, are better resolution, and uncertainty estimates, of absolute velocities and velocity-depth gradients. Better theoretical approximations (e.g., including finite frequency effects and off-great circle wave propagation [44–46]) can improve anomaly amplitude recovery, as well as provide a more realistic spatial resolution estimate. The inferred absolute velocity can also be significantly affected by damping towards a reference model, and in the several-stage surface-wave inversions, by limiting the search space of path-average velocity models. Such procedures are unavoidable, but repeating the analysis for a set of reference models allows for a better characterization of the uncertainties in absolute velocity [47].

The uncertainties in absolute velocity also translate into uncertainties in velocity-depth gradients. The surface waves employed in SHMZ02 and YK04 are relatively sensitive to velocity variations with depth for our depth range of interest (compared to e.g., teleseismic travel times). To include higher frequency surface waves, which have more depth sensitivity, would require better theoretical approaches and corrections for scattering. Additional data that improve lateral resolution may also enhance vertical resolution (e.g., regional body waves), but will probably not lead to much refinement of the current 50 km depth resolution. Uncertainty estimates of the seismically recovered depth gradients can be improved, by statistical analyses of the properties of acceptable velocity structures [48]. In addition, forward tests of the compatibility of proposed physical structures with seismic data can help to evaluate plausible interpretations (e.g., [36,37]).

4.2. Crustal vs. mantle heat flux

Our Australian continental geotherms show that thermo-tectonic age may play some role in controlling the background thermal regime, distinguishing Precambrian from Phanerozoic regions (Fig. 3). However, the large regional variability indicates that tectonic age alone is a poor temperature indicator on anything but the very largest scale.

Variations in crustal heat production have often been designated as the main control on such regional variations [5,49]. Fig. 5 illustrates the sensitivity of lithospheric temperature to crustal and mantle heat-flow variations by abandoning the 0.6 q_s correlation between surface and mantle heat flow assumed in the theoretical geotherms [after 6] plotted in Figs. 2–4. Conductivity parameters are from [6]. Profiles were calculated for fixed mantle heat-flow values, of 10, 15, 20 and 40 mW/m^2, while upper crustal heat production at the surface was tailored to obtain total surface heat-flow values compatible with the most commonly measured values, between 40 and 90 mW/m^2. Heat production decreases exponentially with depth in the upper crust, with a characteristic depth of 15 km. Lower crustal heat production is set to a constant value of 0.22 μW/m^3 [7]; heat production below the crust is set to zero.

These calculations show that crustal heat production variations produce lithospheric temperature deviations of just a few hundred degrees (Fig. 5). A strong accumulation of heat-producing elements in the deep crust may produce a somewhat larger lithospheric temperature range [49], but only by a few tens to a hundred degrees for upper-crustal depth distributions of heat production ranging from exponential to linear, and

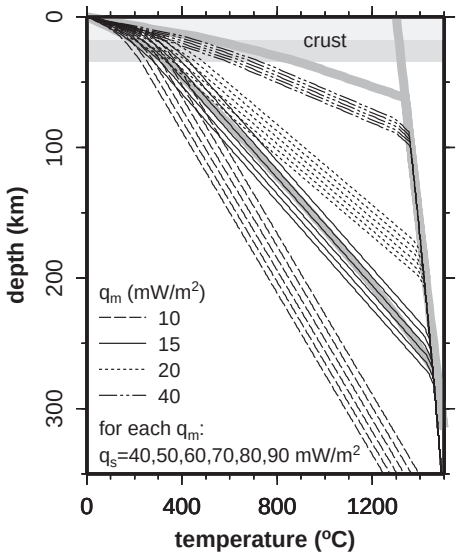

Fig. 5. Theoretical steady-state conductive geotherms for fixed mantle heat-flow values and a range of crustal heat production to obtain total surface heat-flow values (q_s) of 40, 50, . . ., 90 mW/m^2. Parameter values are given in the text. Curves are shown for a mantle heat flux of 10, 15, 20 and 40 mW/m^2 (for the latter no q_s=40 mW/m^2 geotherm is shown). For reference, the 40 and 90 mW/m^2 geotherms according to [6], and a 1300 °C adiabat (which limits conductive temperatures) are shown in bold gray lines. It is clear that variations in mantle heat flow induce much larger temperature variations in the subcrustal lithosphere than variations in crustal heat production. Different depth distributions of crustal heat production than assumed here have a relatively minor effect on the total lithospheric temperature spread.

lower crustal heat production within the range of [7]. Most observations, including those for Australia, point to shallow crustal concentrations [6,16,17,32,50]. Thus, the large range of seismically estimated lithospheric temperatures requires significant variations in heat flux from below the crust.

Although the thermal gradients are not a well-constrained part of the seismic models, it is interesting to note that between 80 and 140 km, our estimated mantle heat flow ranges from close to 0 to 40 mW/m^2 (assuming a mantle conductivity of 3 W/m/K), with the largest variations in the thicker thermal lithosphere of the western two-thirds of the continent. This range is much larger than predicted by dynamic models that find that stable continents buffer the mantle heat flux component to 15 ± 5 mW/m^2 [49,51]. Mantle heat-flow values ranging from 10 to 20 mW/m^2 would put the largest range of temperatures at 200–250 km depth (Fig. 5), assuming steady-state conditions. The observed maximum variation in temperature occurs between 50 and 150 km (Fig. 2). Furthermore, mantle heat-flow values lower than 15 mW/m^2 yield lithospheric thicknesses (Fig. 5) that are larger than the maximum of 300 km inferred from the Australian seismic models.

Lithospheric temperatures under other continents, mapped seismically and inferred from xenolith and heat-flow data, span a similarly large range, also with maximum variability at depths between 50 and 150 km, and thermal thicknesses less than 300 km [7,10,28,32,37,52–54]. Thus, the depth distribution and range of seismically constrained lithospheric temperatures all indicate that mantle heat flux is more variable than dynamic models have predicted. Possibly, small-scale convection, which is suppressed in many models but can affect lithospheric structure [3,55], plays a role in causing variability in heat flow into the base of the crust.

5. Conclusions

A conversion of shallow mantle *S*-velocities under Australia (from models of Simons et al. [21] and Yoshizawa and Kennett [23] between 80 and 350 km depth) to temperature [following [10,27]] gives a first-order picture of subcontinental mantle temperatures that is compatible with thermal structure inferred from surface heat flow and geothermobarometry. Comparison of the results from the two velocity models indicates that more detailed thermal interpretation would require: improved resolution on depth gradients, constraints on reference models and smaller-scale spatial resolution. Although there is an average trend of increasing temperature with decreasing thermo-tectonic age, the variability in thermal structure within tectonic domains is equally large. Within the seismic resolution, the temperatures and lithospheric depths of the Australian Archean and Proterozoic cratonic blocks cannot be distinguished, but they are significantly cooler than those of the Phanerozoic terranes (with or without the imprint of Cenozoic volcanism). The large range in lithospheric temperatures is compatible with the range in seismic temperatures that has been inferred for other continents [10,28,37,52,53], and requires

significant variations in both crustal heat production and mantle heat flow, under conditions that may not be steady-state.

Acknowledgments

We thank Nikolai Shapiro and Sandra McLaren for their thoughtful reviews. This work was supported by the Swiss National Fonds. This is contribution 1388 of the Institute of Geophysics, ETH Zurich.

References

[1] A. Lenardic, L. Moresi, Heat flow scaling for mantle convection below a conducting lid: resolving seemingly inconsistent modeling results regarding continental heat flow, Geophys. Res. Lett. 28 (7) (2001) 1311–1314.
[2] M. Gurnis, Large-scale mantle convection and the aggregation and dispersal of supercontinents, Nature 332 (1988) 695–699.
[3] N.H. Sleep, Survival of Archean cratonal lithosphere, J. Geophys. Res. 108 (B6) (2003) 2302, doi:10.1029/2001JB000169.
[4] H.N. Pollack, D.S. Chapman, On the regional variation of heat flow, geotherms and lithospheric thickness, Tectonophysics 38 (1977) 279–296.
[5] C. Jaupart, J.C. Mareschal, The thermal structure and thickness of continental roots, in: R.D. van der Hilst, W.F. McDonough (Eds.), Composition, Deep Structure and Evolution of Continents, Developments in Geotectonics, vol. 24, Elsevier, Amsterdam, 1999.
[6] D.S. Chapman, Thermal gradients in the continental crust, in: J.B. Dawson, D.A. Carswell, J. Hall, K.H. Wedepohl (Eds.), The Nature of the Lower Continental Crust, Geol. Soc. Spec. Publ., vol. 24, Geol. Soc. London, London, U.K., 1986, pp. 63–70.
[7] R.L. Rudnick, W.F. McDonough, R.J. O'Connell, Thermal structure, thickness and composition of continental lithosphere, Chem. Geol. 145 (1998) 395–411.
[8] W.L. Griffin, S.Y. O'Reilly, C.G. Ryan, O. Gaul, D.A. Ionov, Secular variation in the composition of subcontinental lithospheric mantle: geophysical and geodynamic implications, in: J. Braun, J. Dooley, B. Goleby, R. van der Hilst, C. Klootwijk (Eds.), Structure and Evolution of the Australian Continent, Geodynamics Ser., vol. 26, AGU, Washington, D.C., 1998, pp. 1–26.
[9] T.H. Jordan, Structure and formation of the continental tectosphere, J. Petrol. (1988) 11–37 (Special Lithosphere Issue).
[10] S. Goes, R. Govers, P. Vacher, Shallow upper mantle temperatures under Europe from P and S wave tomography, J. Geophys. Res. 105 (11) (2000) 11,153–11,169.
[11] D.E. James, F.R. Boyd, D.L. Schutt, D.R. Bell, R.W. Carlson, Xenolith constraints on seismic velocities in the upper mantle beneath South Africa, Geochem. Geophys. Geosystems 5 (1) (2004) Q01002, doi:10.1029/2003GC000551.
[12] L. VanGerven, F. Deschamps, R.D. VanderHilst, Geophysical evidence for chemical variations in the Australian continental mantle, Geophys. Res. Lett. 31 (2004) L17607, doi:10.1029/2004GL020307.
[13] A.M. Forte, H.K.C. Perry, Geodynamic evidence for a chemically depleted continental tectosphere, Science 290 (2000) 1940–1944.
[14] J.H. Sass, A.H. Lachenbruch, Thermal regime of the Australian continental crust, in: M.W. McElhinny (Ed.), The Earth: Its Origin, Structure and Evolution, Academic Press, London, 1979, pp. 301–351.
[15] H.N. Pollack, S.J. Hurter, J.R. Johnson, Heat flow from the earth's interior: analysis of the global data set, Rev. Geophys. 31 (1993) 267–280.
[16] S. McLaren, M. Sandiford, M. Hand, N. Neumann, L. Wyborn, I. Bastrakova, The Hot Southern Continent: Heat Flow and Heat Production in Australian Proterozoic Terranes, in: Evolution and Dynamics of the Australian Plate, R.R. Hillis and R.D. Müller, eds., Geol. Soc. Am. Spec. Pap. 372, Geol. Soc. Aus. Spec. Pub. 22, 2003.
[17] N. Neumann, M. Sandiford, J. Foden, Regional geochemistry and continental heat flow: implications for the origin of the South Australian heat flow anomaly, Earth Planet. Sci. Lett. 183 (2000) 107–120.
[18] S.Y. O'Reilly, W.L. Griffin, O. Gaul, Paleogeothermal gradients in Australia: key to 4-D lithosphere mapping, AGSO J. Aust. Geol. Geophys. 17 (1) (1997) 63–72.
[19] B.L.N. Kennett, Seismic Structure in the Mantle Beneath Australia, in: Evolution and Dynamics of the Australian Plate, R.R. Hillis and R.D. Müller, eds., pp. 7–23, Geol. Soc. Am. Spec. Pap. 372, Geol. Soc. Aus. Spec. Pub. 22, 2003.
[20] E. Debayle, B.L.N. Kennett, The Australian continental upper mantle: structure and deformation inferred from surface waves, J. Geophys. Res. 105 (B11) (2000) 25,423–25,450.
[21] F.J. Simons, R.D. Van der Hilst, J.-P. Montagner, A. Zielhuis, Multimode Rayleigh wave inversion for heterogeneity and azimuthal anisotropy of the Australian upper mantle, Geophys. J. Int. 151 (2002) 738–754.
[22] F.J. Simons, R.D. Van der Hilst, A. Zielhuis, The deep structure of the Australian continent from surface-wave tomography, Lithos 48 (1999) 17–43.
[23] K. Yoshizawa, B.L.N. Kennett, Multimode surface wave tomography for the Australian region using a three-stage approach incorporating finite frequency effects, J. Geophys. Res. 109 (2004) B02310, doi:10.1029/2002JB002254.
[24] S. Fishwick, B.L.N. Kennett, A.M. Reading, Contrasts in lithospheric structure within the Australian craton—insights from surface wave tomography, Earth Planet. Sci. Lett. 231 (2005) 163–176.
[25] S. Van der Lee, G. Nolet, Upper mantle *S*-velocity structure of North America, J. Geophys. Res. 102 (1997) 22,815–22,838.
[26] R. Montelli, G. Nolet, F.A. Dahlen, G. Masters, E.R. Engdahl, S.-H. Hung, Global P and PP travel time tomography: rays vs. waves, Geophys. J. Int. 158 (2004) 637–654.

[27] F. Cammarano, S. Goes, P. Vacher, D. Giardini, Inferring upper mantle temperatures from seismic velocities, Phys. Earth Planet. Inter. 138 (2003) 197–222.
[28] S. Goes, S. Van der Lee, Thermal structure of the North American uppermost mantle inferred from seismic tomography, J. Geophys. Res. 107 (B3) (2002) (2000JB000049).
[29] J.J. Ita, L. Stixrude, Petrology, elasticity, and composition of the mantle transition zone, J. Geophys. Res. 97 (1992) 6849–6866.
[30] F.J. Simons, R.D. Van der Hilst, Age-dependent seismic thickness and mechanical strength of the Australian lithosphere, Geophys. Res. Lett. 29 (11) (2002), doi:10.1029/2002GL014962.
[31] G. Hirth, D.L. Kohlstedt, Water in the oceanic upper mantle: implications for rheology, melt extraction and the evolution of the lithosphere, Earth Planet. Sci. Lett. 144 (1996) 93–108.
[32] I.M. Artemieva, W.D. Mooney, Thermal thickness and evolution of Precambrian lithosphere: a global study, J. Geophys. Res. 106 (8) (2001) 16,387–16,414.
[33] D. McKenzie, M.J. Bickle, The volume and composition of melt generated by extension of the lithosphere, J. Petrol. 29 (1988) 625–679.
[34] I. Jackson, Elasticity, composition and temperature of the Earth's lower mantle; a reappraisal, Geophys. J. Int. 134 (1998) 291–311.
[35] D.H. Green, T.J. Falloon, Pyrolite: a ringwood concept and its current expression, in: I. Jackson (Ed.), The Earth's Mantle: Composition, Structure and Evolution, Cambridge Univ. Press, New York, 1998, pp. 311–378.
[36] F. Cammarano, A. Deuss, S. Goes, D. Giardini, One-dimensional physical reference models for the upper mantle and transition zone: combining seismic and mineral physics constraints, J. Geophys. Res. 110 (B1) (2005) B01306, doi:10.1029/2004JB003272.
[37] N.M. Shapiro, M.H. Ritzwoller, Thermodynamic constraints on seismic inversions, Geophys. J. Int. 157 (2004) 1175–1188.
[38] U.H. Faul, I. Jackson, The seismological signature of temperature and grain size variations in the upper mantle, Earth Planet. Sci. Lett. 234 (2005) 119–134.
[39] S.Y. O'Reilly, W.L. Griffin, 4-D lithosphere mapping: methodology and examples, Tectonophysics 262 (1996) 3–18.
[40] R.M. Allen, G. Nolet, W.J. Morgan, K. Vogfjörd, B.H. Bergsson, P. Erlendsson, G.R. Foulger, S. Jakobsdottir, B.R. Julian, M. Pritchard, S. Ragnarsson, R. Stefánsson, Imaging the mantle beneath Iceland using integrated seismological techniques, J. Geophys. Res. 107 (B12) (2002) 2325, doi:10.1029/2001JB000595.
[41] S. Van der Lee, J.C. VanDecar, M.J. Fouch, D.E. James, Upper mantle structure beneath southern Africa from multidisciplinary constraints, Geophys. Res. Abstr. 5 (2003) 05918.
[42] G. Laske, G. Masters, Constraints on global phase velocity maps from long-period polarization data, J. Geophys. Res. 101 (1996) 16059–16075.
[43] K. Yoshizawa, K. Yomogida, S. Tsuboi, Resolving power of surface wave polarization data for higher-order heterogeneities, Geophys. J. Int. 138 (1999) 205–220.
[44] J. Spetzler, J. Trampert, R. Snieder, The effects of scattering in surface wave tomography, Geophys. J. Int. 149 (2002) 755–767.
[45] K. Yoshizawa, B.L.N. Kennett, Determination of the influence zone for surface wave paths, Geophys. J. Int. 149 (2002) 440–453.
[46] Y. Zhou, F.A. Dahlen, G. Nolet, Three-dimensional sensitivity kernels for surface wave observables, Geophys. J. Int. 158 (2002) 142–168.
[47] N.M. Shapiro, M.H. Ritzwoller, Monte-Carlo inversion of broadband surface wave dispersion for a global shear velocity model of the crust and upper mantle, Geophys. J. Int. 151 (2002) 88–105.
[48] C. Beghein, J.S. Resovsky, J. Trampert, P and S tomography using normal-mode and surface wave data with a neighbourhood algorithm, Geophys. J. Int. 149 (3) (2002) 646–658.
[49] C.M. Cooper, A. Lenardic, L. Moresi, The thermal structure of stable continental lithosphere within a dynamic mantle, Earth Planet. Sci. Lett. 222 (2004) 807–817.
[50] R.L. Rudnick, D.M. Fountain, Nature and composition of the continental crust: a lower crustal perspective, Rev. Geophys. 33 (1995) 267–309.
[51] C. O'Neill, L. Moresi, A. Lenardic, C.M. Cooper, Inferences on Australia's Heat Flow and Thermal Structure from Mantel Convection Modelling Results, in: Evolution and Dynamics of the Australian Plate, R.R. Hillis and R.D. Müller, eds., pp. 169–184, Geol. Soc. Am. Spec. Pap. 372, Geol. Soc. Aus. Spec. Pub. 22, 2003.
[52] A.H.E. Röhm, R.K. Snieder, S. Goes, J. Trampert, Thermal structure of continental upper mantle inferred from S wave velocity and surface heat flow, Earth Planet. Sci. Lett. 181 (2000) 395–407.
[53] S. Van der Lee, S. Goes, Structure of the South American lithosphere–asthenosphere, EOS Trans. Am. Geophys. Un. 81 (48) (2000) F1176.
[54] Y.H. Poudjom Djomani, S.Y. O'Reilly, W.L. Griffin, P. Morgan, The density structure of subcontinental lithosphere through time, Earth Planet. Sci. Lett. 184 (2001) 605–621.
[55] C. Dumoulin, M.P. Doin, L. Fleitout, Heat transport in stagnant lid convection with temperature- and pressure-dependent Newtonian or non-Newtonian rheology, J. Geophys. Res. 104 (B6) (1999) 12,759–12,777.
[56] A.B. Thompson, Water in the Earth's upper mantle, Nature 358 (1992) 295–302.